Position Sensing from Charge Dispersion in Micro-Pattern Gas Detectors with a Resistive Anode

M. S. Dixit [a,d,*], J. Dubeau [b], J.-P. Martin [c] and K. Sachs [a]

[a] *Department of Physics, Carleton University, 1125 Colonel By Drive, Ottawa, ON K1S 5B6 Canada*

[b] *DETEC, Aylmer, QC, Canada*

[c] *Universiy of Montreal, Montreal, QC, Canada*

[d] *TRIUMF, Vancouver, BC Canada*

Abstract

Micro-pattern gas detectors, such as the Gas Electron Multiplier (GEM) and the Micromegas need narrow high density anode readout elements to achieve good spatial resolution. A high-density anode readout would require an unmanageable number of electronics channels for certain potential micro-detector applications such as the Time Projection Chamber. We describe below a new technique to achieve good spatial resolution without increasing the electronics channel count in a modified micro-detector outfitted with a high surface resistivity anode readout structure. The concept and preliminary measurements of spatial resolution from charge dispersion in a modified GEM detector with a resistive anode are described below.

Key words: Gaseous Detectors, Position-Sensitive Detectors, Micro-Pattern Gas Detectors, Gas Electron Multiplier, Micromegas
PACS: 29.40.Cs, 29.40.Gx

1 Introduction

A new class of high-resolution multi-channel gas avalanche micro-detectors has been developed during the past decade for charged particle tracking. The Gas Electron Multiplier (GEM) [1] and the Micromegas [2] are examples of some of

* Corresponding author. Tel.: +1-613-520-2600, ext. 7535; fax: +1-613-520-7546.
Email address: msd@physics.carleton.ca (M. S. Dixit).

the new micro-pattern gas detectors [3] already in wide use. The GEM and the Micromegas sample the avalanche charge using arrays of closely spaced long parallel anode strips to measure a single co-ordinate. Spatial resolutions of 40 to 50 μm are typical with anodes strips at 200 μm pitch. Micro-detectors do require more instrumented channels of electronics than multi-wire proportional chambers. However, the number of readout channels has not yet become an issue for most experiments using micro-detectors for charged particle tracking.

There are potential micro-detector applications, however, where the electronics channel count may become an issue. The Time Projection Chamber (TPC) [4] used in high energy physics experiments is one such example. A single endcap detector is used in the TPC to measure both the radial and the azimuthal co-ordinates of the ionization charge cluster. In the conventional TPC, read out with a multi-wire proportional chamber endcap, the radial co-ordinate is obtained from the anode wire position. A precise second co-ordinate along the anode wire length is measured by sampling the induced cathode charge with a series of several mm wide rectangular pads.

The spatial resolution of a TPC in a high magnetic field is dominated by the $\boldsymbol{E}\times\boldsymbol{B}$ and track angle systematic effects [5,6]. Replacement of the usual anode wire/cathode pad readout with one based on micro-detectors with anode pad readout would almost entirely eliminate the systematics and has the potential to improve the TPC performance significantly. However, the suppression of the transverse diffusion in a high magnetic field may often result in the collection of most of the avalanche charge within the width of a single anode pad resulting in a loss of TPC resolution. For better resolution, a micro-detector readout TPC will need either a finely segmented anode pad structure with a prohibitively large number of instrumented channels of electronics, or perhaps the complication of specially shaped pads which enhance anode charge sharing [7].

We describe here a new technique which can be used to measure the position of a localized charge cluster in a micro-detector using pads of widths similar to those used in wire-pad systems. Most of our tests have so far been done with a modified double-GEM detector. However, the new technique appears to be sufficiently general to be applicable to the Micromegas.

2 Charge dispersion in a micro-detector with a resistive anode

With certain modifications to the anode readout structure, it is possible to measure the position of a localized charge cluster in a micro-detector with pads wider than have been used so far. A thin high surface resistivity film is glued to a separate readout pad plane and is used for the anode (Fig. 1).

The resistive anode film forms a distributed 2-dimensional resistive-capacitive network with respect to the readout pad plane. Any localized charge arriving at the anode surface will be dispersed with the RC time constant determined by the anode surface resistivity and the capacitance density determined by the spacing between the anode and readout planes. With the initial charge dispersed and covering a larger area with time, wider pads can be used for signal pickup and position determination. Features of the new method can be explained by a simple physical model described below.

2.1 A model for charge dispersion in a micro-detector with a resistive anode

The resistive anode and the readout plane together can be looked upon to form a distributed 2 dimensional RC network in the finite element approximation. Consider first the 1 dimensional problem of a point charge arriving at $t = 0$ at the origin in the middle of an infinitely long wire grounded at both ends. For small inductance, the space-time evolution of the charge density ρ on the wire is given by the well-known Telegraph equation:

$$\frac{\partial \rho}{\partial t} = h \frac{\partial^2 \rho}{\partial x^2} \qquad \text{where} \qquad h = 1/RC \ . \tag{1}$$

Here R is resistance per unit length and C the capacitance per unit length for the wire.

The solution for charge density is given by:

$$\rho(x,t) = \sqrt{\frac{1}{4\pi t h}} \exp(-x^2/4th) \ . \tag{2}$$

In analogy with the 1 dimensional case, we can write the Telegraph equation for the case of a resistive surface. At time $t = 0$, a point charge is collected at the origin by a resistive anode surface of infinite radius (for simplicity). The 2-dimensional Telegraph equation for the charge density is:

$$\frac{\partial \rho}{\partial t} = h \left[\frac{\partial^2 \rho}{\partial r^2} + \frac{1}{r} \frac{\partial \rho}{\partial r} \right] \ , \tag{3}$$

where in this case, R is the surface resistivity and C is capacitance per unit area.

The solution for the charge density function in this case is given by:

$$\rho(r,t) = \sqrt{\frac{1}{2th}}\exp(-r^2/4th) \ . \tag{4}$$

The charge density function (equation 4) for the resistive anode varies with time and is capacitively sampled by the readout pads. Fig. 2 shows the time evolution of the charge density for an initially localized charge cluster in a micro-detector with a resistive anode. The charge signal on a pad can be computed by integrating the time dependent charge density function over the pad area. The shape of the charge pulse on a pad depends on the pad geometry, the location of the pad with respect to the initial charge and the RC time constant of the system.

2.2 Charge dispersion signal in micro-detectors with long readout strips

The charge dispersion measurements were carried out with a modified GEM detector with long anode strips. Since a spatial co-ordinate measurement for long strips is meaningful only in a direction transverse to the strip length, we can use the 1-dimensional Telegraph equation (1) to describe the situation. However, the solution for the charge density must account for the finite size of the resistive anode in contrast to the solution given by equation (2) in the long wire approximation.

The boundary conditions to solve equation (1) in this case are:

$$\rho(x=0,t) = \rho(x=s,t) = 0 \ ; \ 0 \leq t \leq \infty \ , \tag{5}$$

where s is the size of the resistive foil (assumed square) held at ground potential along its boundary.

The solution satisfying the finite boundary conditions is:

$$\rho(x,t) = \sum_{m=1}^{\infty} A_m \exp[-(hm\pi/s)^2 t]\sin(xm\pi/s) \ , \tag{6}$$

where the coefficients A_m can be determined from the knowledge of the initial charge density:

$$A_m = \frac{2}{s}\int_0^s \rho(x,t=0)\sin(xm\pi/s)dx \ . \tag{7}$$

The signal on a readout strip can be computed by integrating the charge density function over the strip width. Furthermore, the finite extent of the initial charge cluster, the intrinsic micro-detector charge signal rise time as well as the rise and fall time characteristics of the front-end electronics determine the shape of the measured signal shape. All these parameters need to be included in the model to compare to the experiment.

Model calculations were done for a GEM detector with a resistive anode readout with 1 mm wide strips. The anode resistivity and anode-readout gap in the simulation were chosen to limit the computed spatial spread of the charge dispersion over pads to about 700 μm comparable to transverse diffusion in a high magnetic field TPC. Simulated signals for the readout strip directly below the initial ionization charge cluster and for the next four adjacent strips are shown in Fig. 3. The same figure also shows the simulated pad response function or equivalently the spatial spread of an initially localized charge cluster due to charge dispersion.

3 Spatial resolution measurements in a GEM detector with a resistive anode

The charge dispersion test measurements were made with the modified double-GEM detector (Fig. 1) filled with Ar/CO_2 90/10. A 50 μm thick Mylar film with a surface resistivity of 2.5 MΩ per square was glued to the pad readout board. The spacing between the anode and readout planes was close to 100 μm including the thickness of the glue.

Fig. 4 shows the experimental setup for the space point resolution measurements. The initial ionization is provided by x-ray photon conversion in the gas. The average photon energy was about 4.5 keV as low energy bremsstrahlung photons from the copper target x-ray tube, run at 7 kV, were absorbed by the material in the x-ray tube and detector windows. A $\sim$40 μm pinhole in a thin brass sheet was used to produce a miniaturized x-ray tube focal spot image in the GEM drift gap. The size of the x-ray spot at the detector is estimated to be on the order of 70 μm. After avalanche multiplication and diffusion, the RMS size of the electron cloud reaching the resistive anode was $\sim$400 μm. The gas gain was about 3000.

Signals were read out from 7 cm long and 1.5 mm wide strips. The front-end electronics consisted of Aleph [6] TPC wire charge preamplifiers followed by receiver amplifiers. Signals from 8 contiguous strips were digitized using two 4-channel Tektronix digitizing oscilloscopes. A computerized translation stage was used to move the x-ray spot in small steps over the width of the centre strip. One thousand event runs were recorded for each x-ray spot position on

an event by event basis.

For a given anode surface resistivity and readout geometry, the observed shape of the charge pulse depends on the strip position with respect to the location of primary charge cluster on the resistive anode. Fig. 5 shows an event where the x-ray ionization spot is located directly above the centre of a readout strip. A fast charge pulse is observed on the strip peaking in time with the maximum of the charge density at the anode surface above. Pulses on strips farther away have a slower rise time and peak late because the local charge density on the anode surface nearest the strip reaches its maximum later. Also, an early short duration induced pulse is visible for strips adjacent to the main strip. The induced pulses [8], produced by electron motion in the GEM induction gap, have demonstrated position sensitivity [9] but require the use of high-speed pulse shape sampling electronics. In addition, measurable induced pulses are specific to GEM detectors with sizeable induction gaps. For charge dispersion measurements described below, the induced GEM pulse information has not been used.

4 Data analysis and results

The charge dispersion signals were confined to a narrow region on the readout board in the present setup. There were measurable signals above noise only on three 1.5 mm wide strips. The analysis to determine the space point resolution from the event by event data consisted of following steps: a) Determine the pulse heights of signals on the strips, independent of rise time; b) Compute a centre of gravity position for the event from the measured pulse heights; c) Correct for the bias in the computed centre of gravity to obtain the position of the ionization cluster for the event. The standard deviation of the bias corrected centre of gravity position with respect to the known x-ray beam spot position for the run gives a measure of the space point resolution.

The data from each 1000 event run were sub-divided into two equal data sets: one used for calibration and one for resolution studies. The pulse heights were obtained by fitting polynomial functions to the digitized pulse shape data. The calibration data set was used to determine and fix the coefficients of polynomial functions (see Fig. 6) used subsequently in the analysis of events in the resolution data set.

The centres of gravity for the events in the calibration data set were computed from the measured pulse heights. The correction function for the bias in the centre of gravity method (see Fig. 7) was determined by plotting the mean value of computed centres of gravity against the known x-ray spot position for the individual runs.

The pulse heights and the peak positions for the events used for resolution studies were determined by fitting the pulses to the fixed polynomials shapes obtained from the corresponding calibration data set. The computed centres of gravity were converted to "true position" by interpolation using the bias correction function determined from the calibration data set. Fig. 8 shows the measured resolution function for the 1.5 mm wide strips at two different positions of the x-ray ionization spot over the strip. Fig. 9 shows the measured spatial resolutions and the position residuals: i.e. the deviation of measured positions from the micrometer settings. The small systematic trends apparent in the plot appear to be related to an imprecise knowledge of the experimental parameters in the present setup and any remaining biases in the present method of analysis. Nevertheless, the standard deviations of the position measurements, in the range of 50 to 80 μm, are all consistent with the size of the collimated x-ray spot at the detector.

5 Outlook and summary

We have demonstrated that a controlled RC dispersion of the avalanche charge makes it possible to measure its position with a micro-detector with strips wider than have been used previously. The pad response function and signal shapes are determined by the anode surface resistivity and anode-readout plane gap. With the proper choice of the RC time constant of the system, the charge dispersion technique will not compromise the counting rate ability of the detector. Nor should it compromise the 2-track resolving power of the detector which should be limited only by the diffusion effects in the gas. Once the characteristics of the charge dispersion signal are properly understood, it should also be possible to simplify the technique replacing the pulse shape measurement system with less expensive charge integrating electronics.

The charge dispersion space point resolution studies described here were done for long readout strips in a modified GEM detector with a resistive anode. Further experimental and simulation studies are in progress to investigate the spatial resolution capabilities of the charge dispersion technique with rectangular pads similar to those used in wire-cathode pad TPCs. We are also testing the concept of position sensing from charge dispersion with the Miromegas where the high anode resistance may help improve the detector HV stability as well as protect the front-end electronics from spark damage.

Acknowledgments

The charge preamplifiers used in these measurements came from the Aleph TPC at CERN and we wish to thank Ron Settles for making these available to us. Ernie Neuheimer lent us his expertise in designing, building and troubleshooting much of the specialized electronics used for these measurements. Mechanical engineers Morley O'Neill and Vance Strickland helped with the detector design and in improving the clean-room facility used for the detector assembly. Philippe Gravelle provided technical assistance when needed. Our CO-OP students Alasdair Rankin and Steven Kennedy made significant contributions to all aspects of this research from hardware construction to improving the data acquisition software as well as writing some of the data analysis code. Finally, one of the authors (MSD) would like to express his thanks to V. Radeka for an illuminating discussion concerning the phenomenon of charge dispersion. This research was supported by a project grant from the Natural Sciences and Engineering Research Council of Canada.

References

[1] F. Sauli, Nucl. Inst. Meth. **A386** (1997) 531.

[2] Y. Giomataris et al, Nucl. Inst. Meth. **A376** (1996) 29.

[3] F. Sauli and A. Sharma, Ann. Rev. Nucl. Part. Sci. **49** (1999) 341.

[4] D. R. Nygren, PEP 198 (1975).

[5] C.K.Hargrove et al, Nucl. Inst. Meth. **219** (1984) 461.

[6] S. R. Amendolia et al., Nucl. Inst. Meth. **A283** (1989) 573.

[7] M. Schumacher, LC-DET-2001-014.

[8] M.S. Dixit et al, Proceedings of Workshop on Micro-Pattern Gas Detectors, Orsay France (1999).

[9] D. Karlen et al, Physics and experiments with future linear e^+e^- colliders, LCWS2000, American Institute of Physics Conf. Proc. Vol 578.

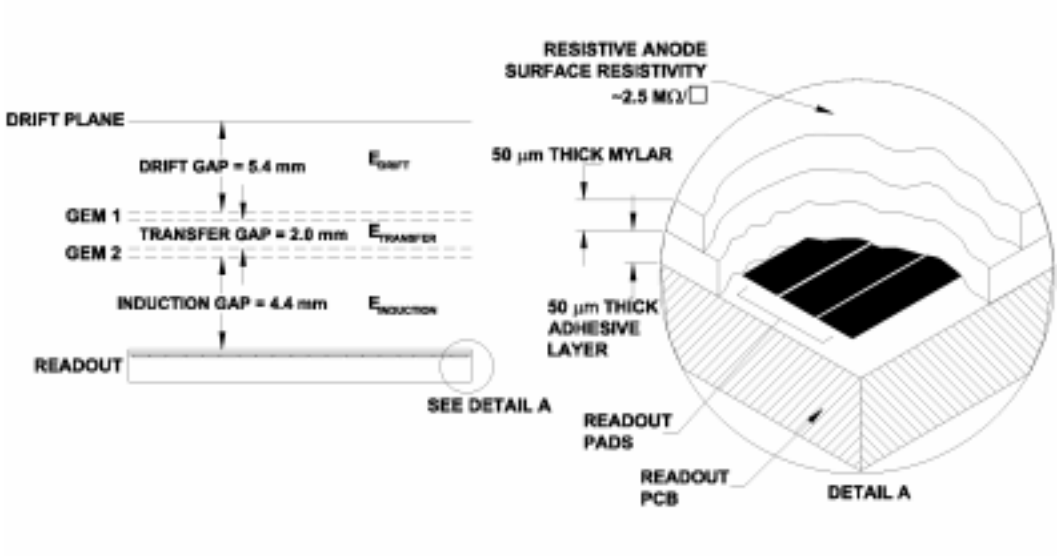

Fig. 1. Schematics of the resistive anode double-GEM detector used for charge dispersion studies.

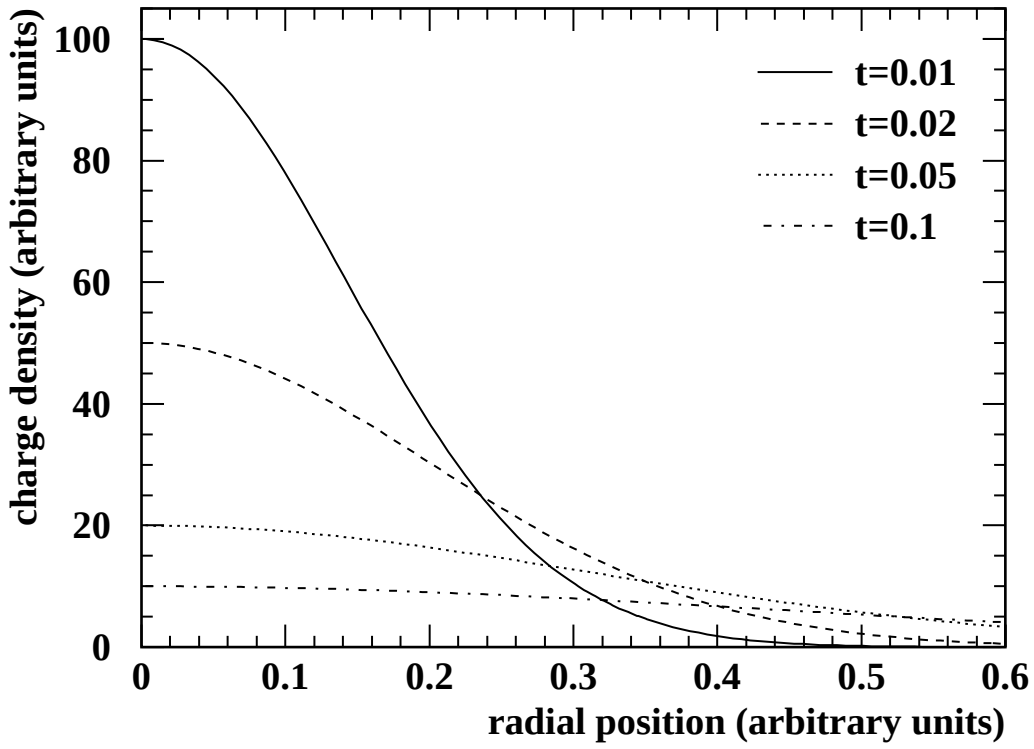

Fig. 2. The evolution of the charge density function on the resistive anode in a micro-detector with increasing time (arbitrary units). The initial charge was point-like and localized at the origin at time = 0.

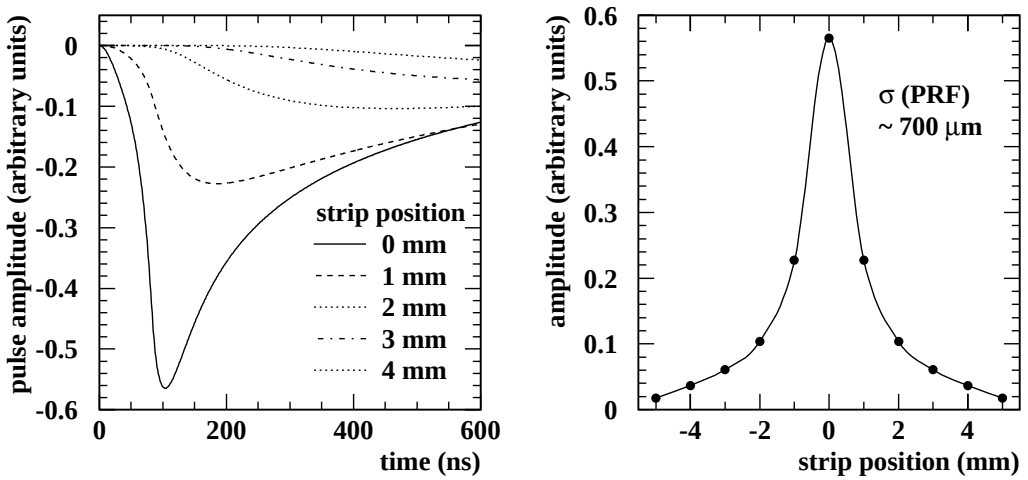

Fig. 3. Simulated signals for 1 mm wide strips assuming an anode resistivity of 2.5 MΩ per square and anode-readout plane separation of 100 μm. The pad response function for charge dispersion is shown on the right. The diffusion effects were neglected for this simulation.

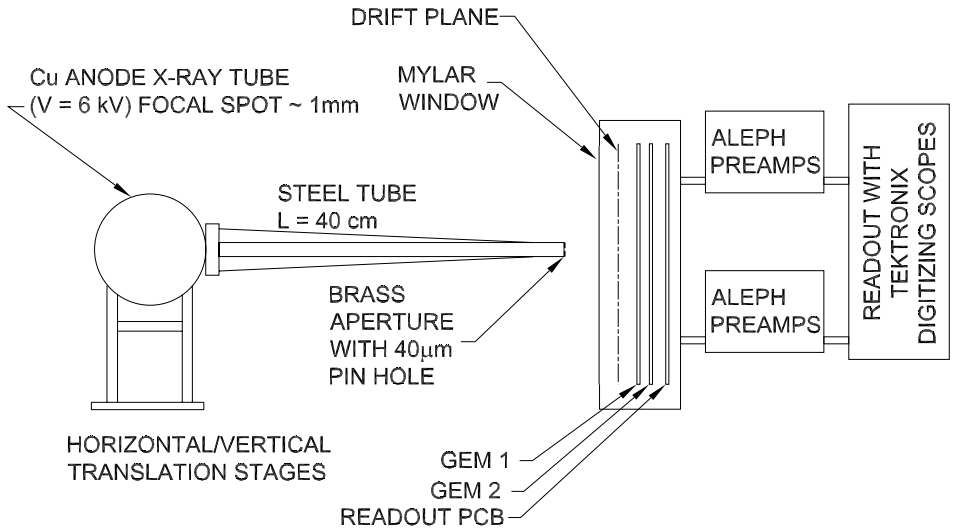

Fig. 4. The experimental setup for the double-GEM resistive anode charge dispersion measurements.

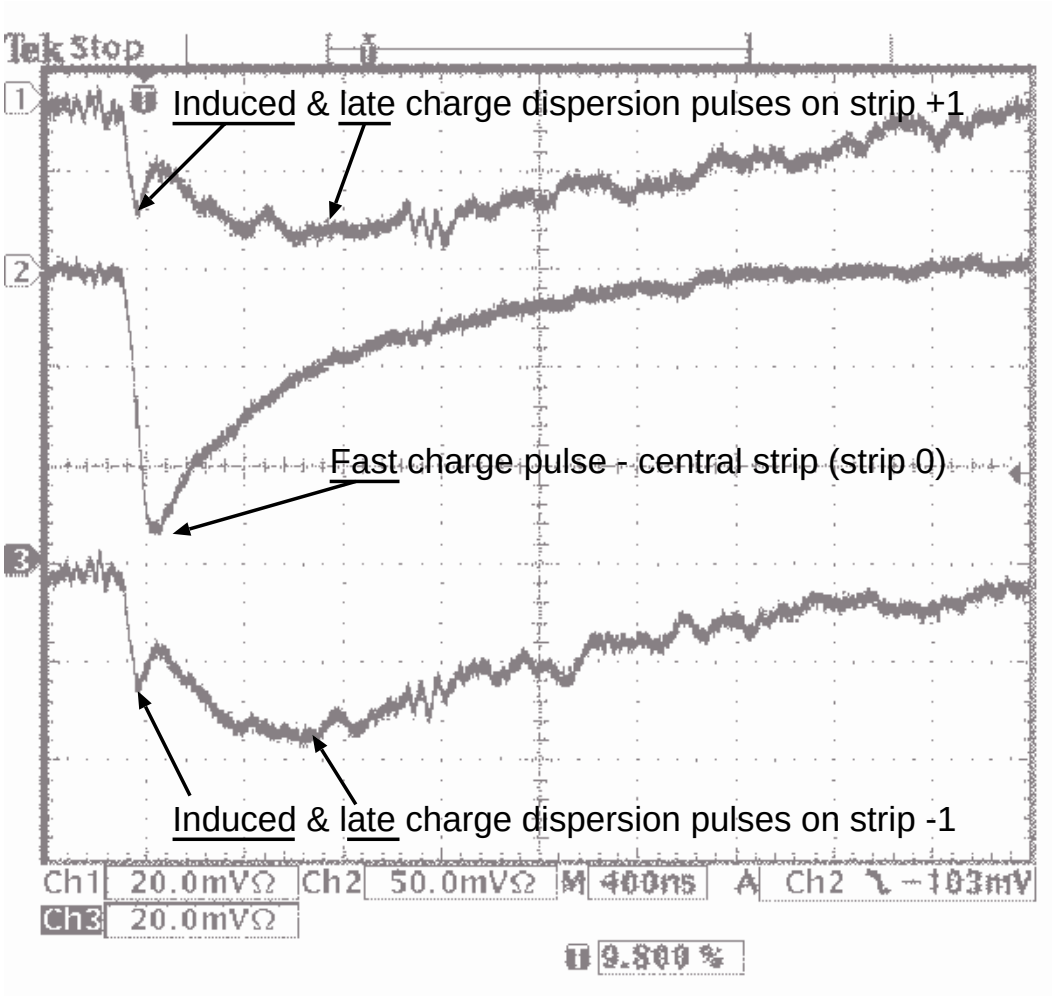

Fig. 5. Observed signals on three adjacent strips for a single x-ray photon conversion in the double-GEM detector.

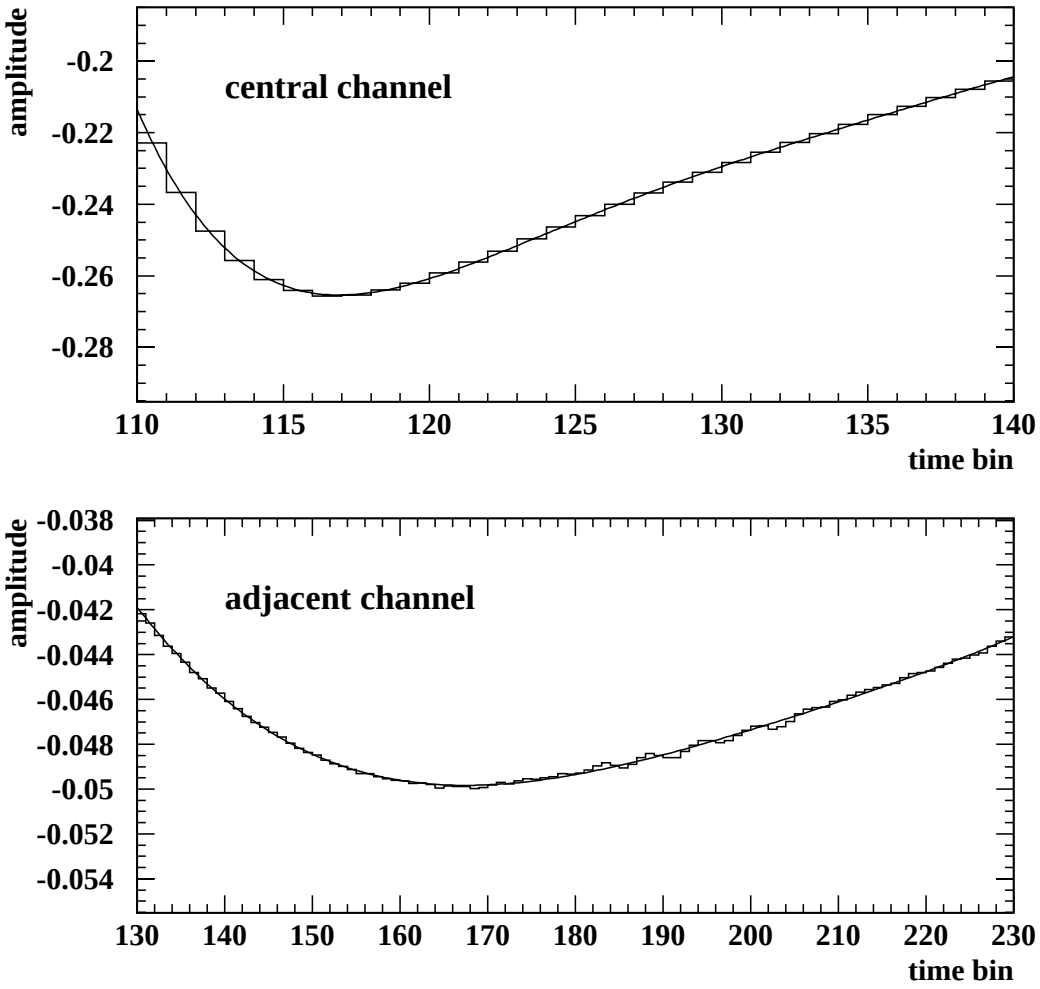

Fig. 6. Polynomials were fitted to the calibration data set for each run to fix the functions used to determine the pulse height of events for resolution studies. The top figure shows the polynomial fit to the average of fast charge pulses for the centre strip. The figure below shows the polynomial fit to the average of late charge dispersion pulses for an adjacent strip.

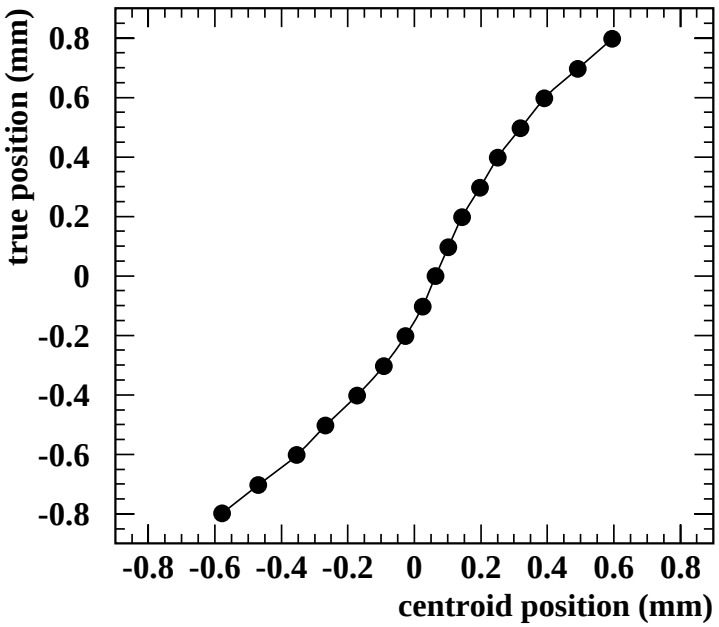

Fig. 7. The bias correction function shown in the figure was experimentally determined. The bias function was used in converting the computed centroid of signals on three strips to the true position on an event by event basis.

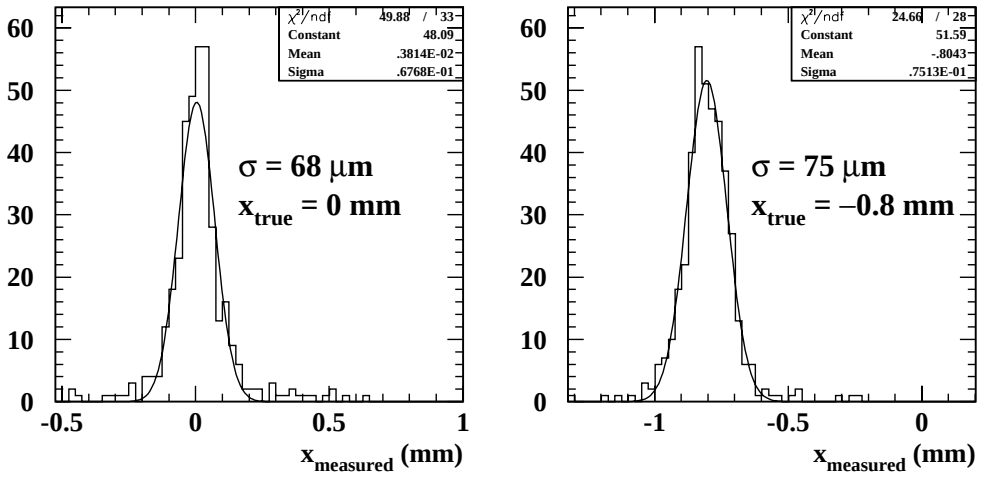

Fig. 8. The resolution function for two x-ray beam spot positions.

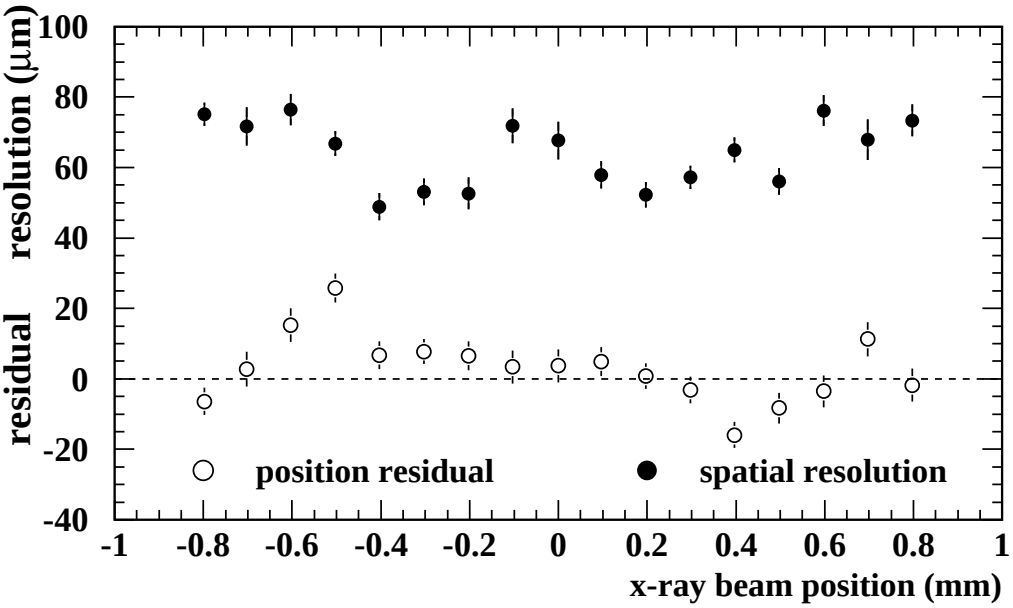

Fig. 9. The summary of the spatial resolutions and the position residuals for the x-ray scan across the readout strips.